

Diffraction analysis and evaluation of several focus- and track-error detection schemes for magneto-optical disk systems

Bruce E. Bernacki and M. Mansuripur

*Optical Sciences Center, University of Arizona
Tucson, Arizona 85721*

ABSTRACT

A commonly used tracking method on pre-grooved magneto-optical (MO) media is the push-pull technique, and the astigmatic method is a popular focus-error detection approach. These two methods are analyzed using DIFFRACT[®], a general-purpose scalar diffraction modeling program, to observe the effects on the error signals due to focusing lens misalignment, Seidel aberrations, and optical crosstalk (feedthrough) between the focusing and tracking servos. Using the results of the astigmatic/push-pull system as a basis for comparison, a novel focus/track-error detection technique that utilizes a ring toric lens is evaluated as well as the obscuration method (focus error detection only).

1. INTRODUCTION

To achieve the highest recording densities promised by MO storage technology, it is essential that the axial position of the focusing lens that forms the optical stylus for thermo-magneto-optic recording and readout be held within tight tolerances. These tolerances result from the compromise between the high numerical aperture (NA) required to produce the smallest diffraction-limited spot size for high areal recording densities, and the low NA desired for a large depth of focus. Adding to this challenge is the requirement to move the optical head across the rotating disk to seek the desired track, and then, to maintain the head position on the correct track.

Although the tasks of focusing and tracking seem daunting, there is a plethora of focus error detection and tracking schemes from which to choose. In this paper, the astigmatic focus error detection method is studied in depth, along with the push-pull tracking method used on grooved MO media. The study is further broadened to include a novel focus error detection method using a ring toric lens, which may be used in conjunction with the push-pull tracking method. Additionally, the obscuration method for focus error detection is studied and comparison made with the other techniques.

2. METHODOLOGY/TOOLS

Each system is first modeled in its ideal form. The system is then perturbed to examine the effects of third-order aberrations, focusing lens misalignment and feedthrough. For this study, we define feedthrough as the unwanted focus error signal (FES) that is detected when the optical head is crossing the tracks, with the head held in nominal focus. The astigmatic/push-pull system is examined first since it is more familiar.

The computer tools used in this study have been described in detail elsewhere¹. DIFFRACT[®] is a diffraction modeling program written in FORTRAN that was created as a general-purpose tool for optical data storage research. The user has a palette from which many types of lenses, polarization optics, media, and detectors encountered in optical data storage may be selected. DIFFRACT[®] permits the user to choose a uniform or truncated Gaussian amplitude distribution produced by a

collimated laser source, and then propagates this beam through the optical system by plane wave decomposition and Fourier methods. The polarization state and the intensity distribution of the propagating beam, as well as various detector outputs are available anywhere along the optical path during the simulation. The right-handed Cartesian coordinate system is used throughout this study, with the propagation of light taken to be in the +z direction. Positive angles are measured counter-clockwise with respect to the positive x-axis.

3. SYSTEM LAYOUT

In common with all the focusing and tracking techniques studied, the initial amplitude distribution is a collimated Gaussian laser beam with $\lambda = 800$ nm, $1/e$ radius of 3.2 mm and zero curvature. This beam is truncated by a 0.55 NA objective lens with focal length 3.76 mm: the truncated beam radius is 2.07 mm. A pre-grooved disk with rectangular cross section lies in the focal plane of the objective lens with groove geometry as follows: 1.6 μ m pitch, 80 nm groove depth, 0.6 μ m groove width, and 1.0 μ m land width. The focused spot is reflected from the disk surface, and, 20 mm from the objective, the focus/track error detection components are positioned. For simulations of the non-ideal system, aberrations were introduced in the objective lens. Aberrations with angular pupil dependence were oriented to produce worst-case effects: coma was oriented 90° to the track direction, and astigmatism was oriented such that the sagittal and tangential foci were 45° to the track direction. Misalignments were treated by simulating the movement of the objective lens perpendicular to the groove direction.

4. SYSTEM SIMULATION RESULTS

4.1 Astigmatic focusing/push-pull tracking method

The theoretical background is well documented in the literature^{2,3}, hence, the technique, shown in Fig. 1, will only be described schematically. Light reflected from the disk is collected by an astigmat, i.e., a lens with two orthogonal line foci. A quadrant detector is placed between the two foci. For these simulations, $f_1 = 19.75$ mm and $f_2 = 20.25$ mm. The quadrant detector is treated as an ideal device with no dead zone between the quadrants. The orientation and numbering of the quadrants are as shown in Fig. 1.

The operation of the servo is readily understood using geometrical optics.⁴ When the disk lies in the focal plane of the objective lens, the circle of least confusion coincides with the position of the quadrant detector, and light falls symmetrically on all four quadrants. However, when the light returning from the disk surface begins to diverge or converge due to disk movement in the $\pm z$ -direction, the location of the circle of least confusion changes, and the intensity pattern on the the quadrant detector becomes elliptical, with the major axis of the ellipse corresponding to the nearer line focus of the astigmat. The error signal is obtained from the following combination of detector signals:

$$FES = \frac{(I+III) - (II+IV)}{I+II+III+IV} \quad (1)$$

Its ultimate sensitivity depends inversely¹ on the separation of the astigmatic foci. The result is a

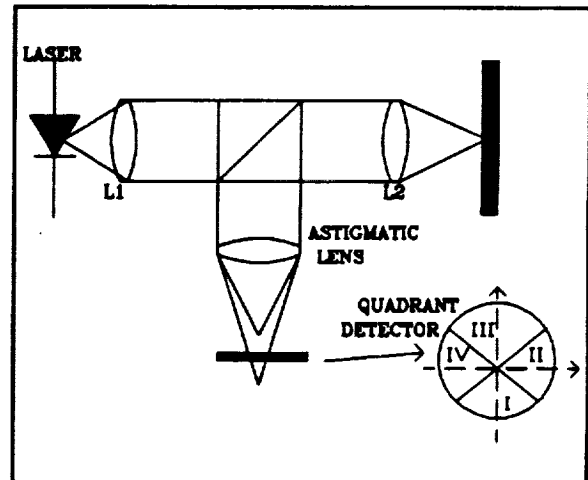


Figure 1. Layout for astigmatic focusing-push-pull tracking method showing geometry of quadrant detector.

bipolar error signal as shown in the solid curve of Fig. 2. Here, we define defocus as the amount of disk displacement from the focal plane of the objective lens along the $\pm z$ -direction. The focal plane coincides with the $z=0$ position. The gain G is the figure of merit for focus error detection systems and is defined here as the slope of the FES curve.

To understand the effect of Seidel aberrations on the FES, consider the nature of aberration present: Is it even or odd? Odd aberrations, e.g. coma, mimic the off-track condition and do little to degrade the FES since they produce a common mode signal on the quadrant detector. Even aberrations, such as spherical aberration, behave like defocus, causing the FES to be offset, as can be seen in Fig. 2. In practice, the offset caused by the even aberrations is nulled electronically or optically as part of a calibration procedure. The figure of merit, G , for this system is 0.16.

The operation of push-pull tracking can be understood by considering the disk surface as a reflective grating and observing its far-field diffraction pattern.³ When the focused beam is exactly on track, diffraction from the edges of the land is symmetric, causing the far-field diffraction pattern to be symmetric. However, as the spot moves across the track, light from the 0 and ± 1 orders is diffracted unequally from groove/land edges and destroys the symmetry of the far-field pattern, skewing the intensity distribution perpendicular to the groove direction. The orientation of the astigmat also causes the intensity distribution to be rotated 90°. The result is a bipolar track error signal (TES) as seen in Fig. 3 that is obtained from the quadrant detector using the relationship

$$TES_{\text{quad}} = \frac{(I+IV) - (II+III)}{I+II+III+IV} \quad (2)$$

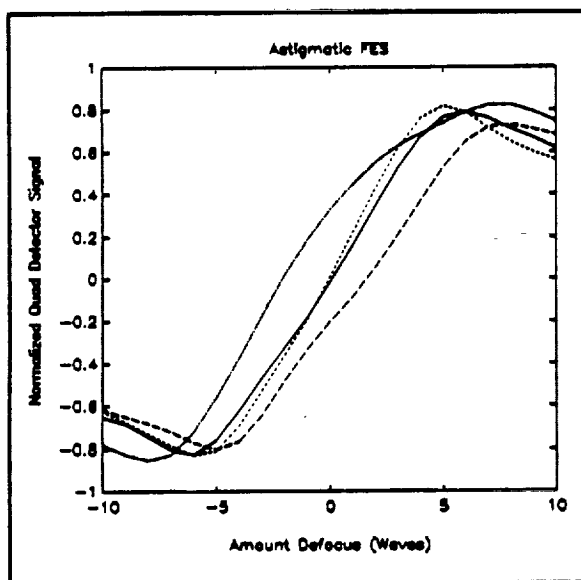


Figure 2. Astigmatic FES. No aberrations (solid), $+0.25 \lambda$ spherical aberration (dash), $+0.25 \lambda$ astigmatism (dash-dot), and $+0.25 \lambda$ coma (dot).

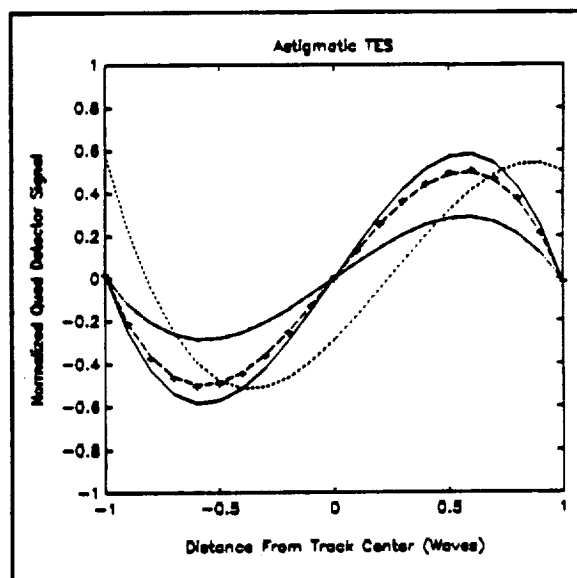


Figure 3. Astigmatic TES. No aberration (solid), $+0.25 \lambda$ spherical aberration (dash), $+0.25 \lambda$ astigmatism (dash-dot), $+0.25 \lambda$ coma, (dot), and $+1 \lambda$ defocus (+).

For the push-pull TES, defocus reduces the slope of the signal, seen above in Fig. 3. Since the grating structure produces interference between the 0 and ± 1 orders, it is a grating-type lateral shearing interferometer⁴. Therefore, an even aberration like defocus will produce a system of straight line fringes where the 0 and ± 1 orders overlap, which reduces the contrast at the detector, and diminishes the slope of the TES. For the odd aberration studied, coma, the comatic tail was oriented in its worst-case orientation: perpendicular to the track direction. Its effect is to produce an offset in the TES, while maintaining the slope. As was the case with the FES, the reduced slope of the TES could be compensated by increasing the gain of the servo or adding some defocus to minimize

spherical aberration, while the offset of the zero crossing due to coma can be nulled by a corresponding electronic offset in the servo circuitry.

The fine adjustment of lens positioning used in tracking (usually accomplished using a voice coil arrangement) causes the lens to be displaced from the optical axis of the input beam by as much as $\pm 50 \mu\text{m}$. The effect of this operation on the TES was investigated by displacing the lens 0, 10, and 24λ from the optical axis of the system along a line perpendicular to the groove direction. Then, the disk was scanned $\pm 1 \lambda$ about the center of the original system, and the TES calculated. Moving an even number of waves puts the beam on a land center for this disk geometry. The results of the simulations, seen in Fig. 4, show that fairly good track error signals result for these amounts of lens decentering. No effect on the FES could be detected using these decentering values.

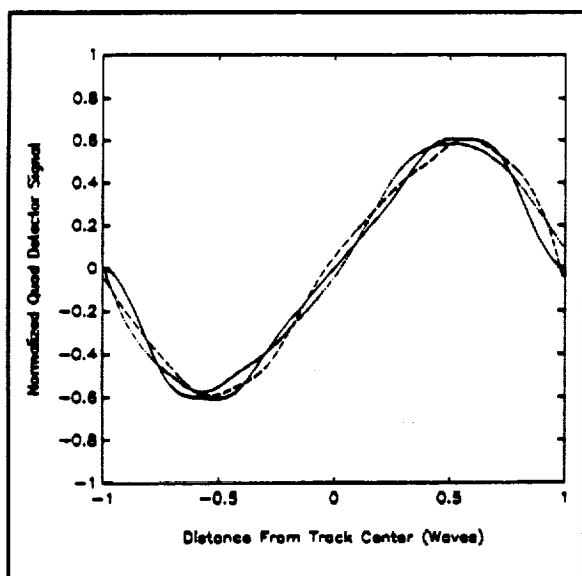


Figure 4. Astigmatic TES with lens decentering of 0 (solid), 10λ (dash), and 24λ (dash-dot) perpendicular to track direction.

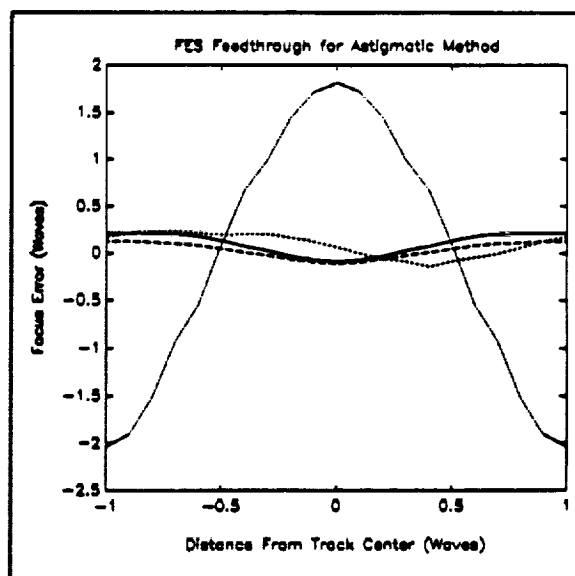


Figure 5. FES feedthrough for astigmatic method. No aberrations (solid), $+0.25 \lambda$ spherical aberration (dash), $+0.25 \lambda$ astigmatism (dash-dot), and $+0.25 \lambda$ coma (dot).

Feedthrough is the unwanted FES that is detected when the optical head is seeking a new track. Ideally, the TES and FES should not be coupled. The reality of the situation is shown in Fig. 5. The focus error was calculated by determining the slope of the best fit line to the linear portion of the solid FES curve in Fig. 2, defined as G , and then its reciprocal was used to determine the error in the focus servo that results due to feedthrough. For feedthrough measurements, best focus was found to maximize the Strehl ratio for spherical aberration. In this case, the Strehl ratio improved from 0.81 uncompensated, to 0.98 with defocus added. The maximum 0.25λ peak-to-peak error in the case of no aberration, coma, and spherical aberration could be tolerated by a well-designed control system, and any DC offsets in the signal can be nulled electronically. However, the 3.5λ peak-to-peak focus error due to $+0.25 \lambda$ of astigmatism oriented such that the astigmatic foci are 45° to the track would be intolerable, and therefore must be avoided in practice.

4.2 Ring toric lens/push-pull method

A focus- and track-error detection scheme has been described⁵ that employs a ring toric lens and a four cell Φ detector, shown in Fig. 6. The Φ detector takes its name from the shape of the Greek letter suggested by the segmentation of the detector. The ring toric lens is the optical equivalent of a lens-axicon^{6,7} combination. Collimated light is focused to a diffraction-limited ring

in the focal plane of the ring toric lens.

When the objective lens is in focus, the ring focus is centered on the dashed circle of the Φ detector. Diverging light returning from the disk surface shifts the ring focus outside the dashed circle shown in Fig. 6, while converging rays shift the ring focus inside the dashed circular area of the Φ detector. Unlike the astigmatic FES method, the ring toric approach is diffraction-limited, and its FES would approach a step function in the geometrical optics limit. Its slope is finite due to diffraction, however. The FES for the ring toric method, shown in Fig. 7, has $G=0.42$ and is obtained from the four-cell Φ detector by the following relation

$$FES_r = \frac{(I+II)-(III+IV)}{I+II+III+IV} \quad (3)$$

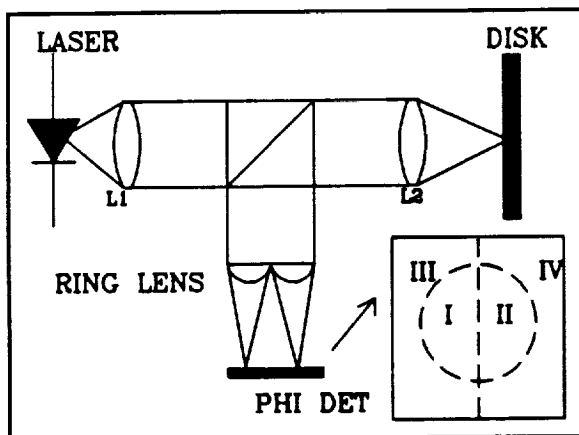


Figure 6. Ring toric lens method showing four-cell Φ detector. Focal length 25000λ , inner ring radius 50λ , outer ring radius 2750λ , radius of ring in Φ detector 100λ .

As was the case with the astigmatic method, the even aberrations have the greatest effect on the FES, since their behavior is similar to defocus, and offset the zero crossing. Also, since the gain G of the ring toric method is diffraction-limited, the presence of small amounts of even aberrations reduce its sensitivity as well as causing an offset.

Push-pull tracking is accomplished with the ring toric lens by summing the following regions of the Φ detector

$$TES_r = \frac{(I+III)-(II+IV)}{I+II+III+IV} \quad (4)$$

The performance of the TES produced by the ring toric, including the effects of focusing lens displacement, is indistinguishable from that developed by the astigmatic lens approach.

With the exception of astigmatism, to which the astigmatic method is understandably more sensitive, the focus feedthrough signals are nearly equivalent in the two methods. However, since the focus error produced is proportional to $1/G$, the greater gain of the ring toric method reduces the magnitude of the focus error due to feedthrough, as can be seen in Fig. 8. Best focus was also found to maximize the Strehl ratio, as was done for the astigmatic method.

4.3 Obscuration method

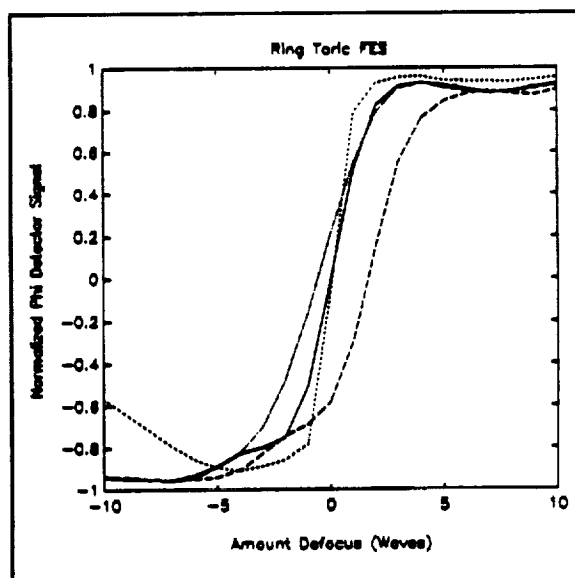


Figure 7. Ring toric FES. No aberrations (solid), $+0.25 \lambda$ spherical aberration (dash), $+0.25 \lambda$ astigmatism (dash-dot), and $+0.25 \lambda$ coma (dot).

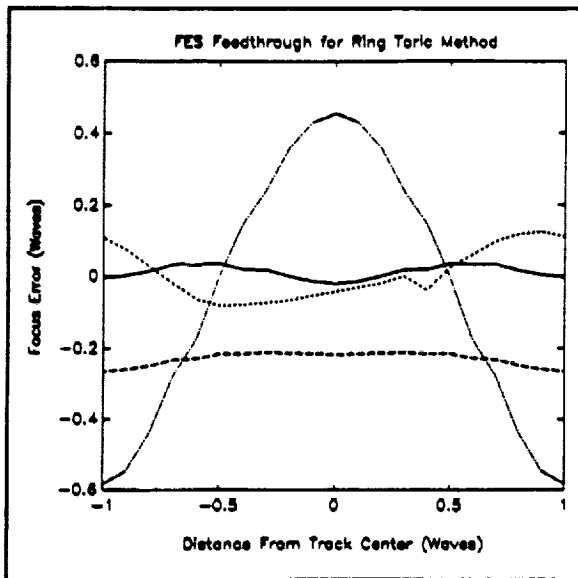


Figure 8. FES feedthrough for ring toric method. No aberrations (solid), $+0.25 \lambda$ spherical aberration (dash), $+0.25 \lambda$ astigmatism (dash-dot), $+0.25 \lambda$ coma (dot).

In this technique (a variation of the Foucault knife edge method) an obscuration is placed against the secondary lens which produces the focus error signal.^{2,3} A split detector placed in the focal plane of the secondary lens produces a differential signal that is highly sensitive to movement of the centroid of the focused spot. Fig. 9 shows the schematic layout for this technique.

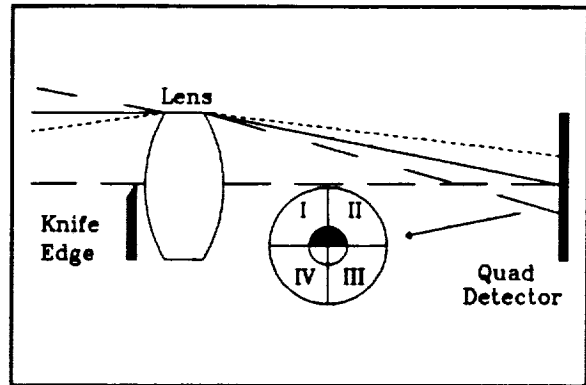


Figure 9. Layout for obscuration focus error detection method.

An out-of-focus condition causes the spot on the detector to move perpendicular to the orientation of the obscuration edge. In the limit of geometrical optics, the FES response approaches a step function, as was the case for the ring toric lens. The slope of the computed FES curve shown in Fig. 10 is due to diffraction. A drawback of this method is the loss of 50% of the light reflected from the disk due to the obscuration in the return path.

Since the obscuration method is diffraction-limited, its performance is similar to the ring toric method with regard to the Seidel aberrations, as can be seen in Fig. 10. Because of its high value of $G = 0.32$, it appears to be nearly as resistant to feedthrough as the ring toric lens method, as is seen in Fig. 11. Note, however, the greater peak-to-peak feedthrough signals in the cases of no aberration, coma, and spherical aberration. Push pull tracking may be done with this method if two Fresnel bi-prisms are employed to split the exit pupil of the secondary lens, or a double wedge-roof prism arrangement⁸ is employed, but these variations were not investigated.

5. SUMMARY

Three focus/track error detection systems were examined in detail in this study: astigmatic/push-pull, ring toric/push-pull, and obscuration method for focus error detection only.

The astigmatic focus servo has a geometrical optics performance limit in the FES, which is degraded by the even Seidel aberrations, but insensitive to odd aberrations. The effect of the even aberrations is to offset the zero crossing of the FES response curve while maintaining nearly the same gain of $G=0.16$. With the exception of astigmatism, peak-to-peak error in the focus servo is less than 0.25λ . However, $+0.25 \lambda$ of astigmatism oriented such that the sagittal and tangential foci are at 45° to the track direction induces a focus error of nearly 4λ peak-to-peak.

Push-pull tracking is degraded by both even and odd aberrations, including defocus. The even aberrations reduce the slope of the TES, but do not shift the zero crossing. The odd aberrations shift the location of the zero crossing, but the slope is preserved. Displacement of the objective lens from the optical axis, which occurs during tracking, was shown to have a small effect on the TES for the aberration-free, in-focus case.

The ring toric focus error detection method has diffraction-limited performance, which produces a steep FES curve and high value of $G=0.42$. It is much less prone to feedthrough than the

astigmatic/push-pull method when astigmatism with worst-case orientation is present. The performance of push-pull tracking with the ring toric lens is identical with that of the astigmatic approach.

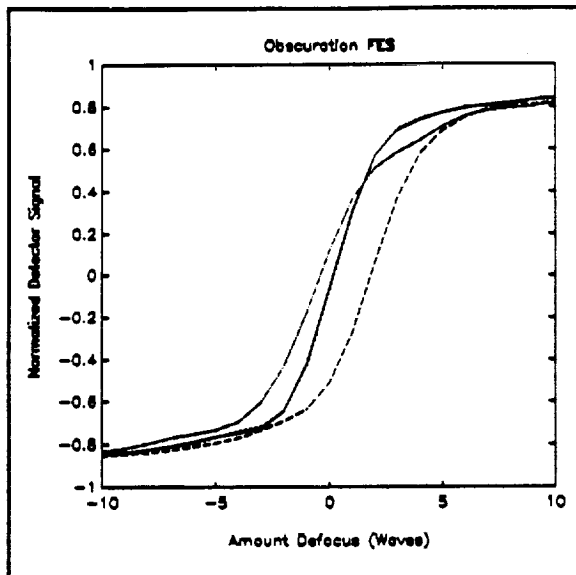


Figure 10. FES for obscuration method. No aberrations (solid), $+0.25 \lambda$ spherical aberration (dash), $+0.25 \lambda$ astigmatism (dash-dot), and $+0.25 \lambda$ coma (dot).

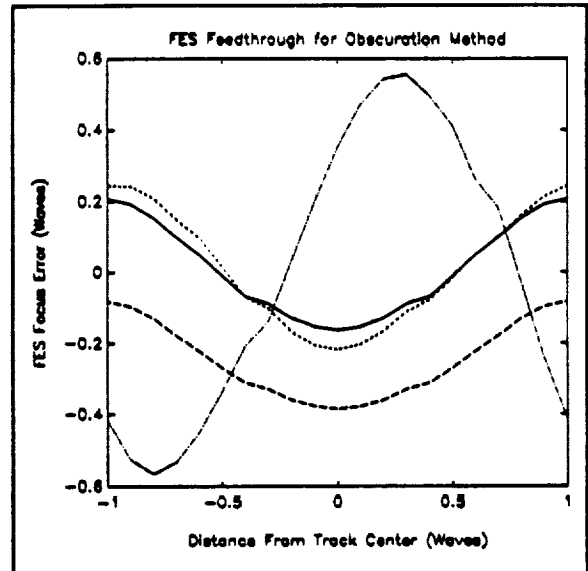


Figure 11. FES feedthrough for the obscuration method. No aberrations (solid), $+0.25 \lambda$ spherical aberration (dash), $+0.25 \lambda$ astigmatism (dash-dot), and $+0.25 \lambda$ coma (dot).

The obscuration method is also diffraction limited, and with $G=0.32$, performs similarly to the ring toric method for focus error detection with regard to its behavior in the presence of aberrations, but performs somewhat worse than the ring toric method with respect to feedthrough. However, its use of the light returned from the disk is inefficient, since half of the lens must be blocked, unlike the astigmatic and ring toric methods, which use all of the available light. Push-pull tracking is possible only in the Fresnel bi-prism implementation of this method.

6. ACKNOWLEDGEMENTS

The authors wish to thank Dr. David Kay of Kodak Research Labs for helping us understand feedthrough in MO disk systems. Bruce Bernacki is supported by a Graduate Assistance in Areas of National Need (GANN) fellowship.

7. REFERENCES

1. M. Mansuripur, "Analysis of astigmatic focusing and push-pull tracking error signals in magneto-optical disk systems," *Appl. Opt.*, 26, No. 18, pp. 3981-3986, 1987.
2. G. Bouwhuis, J. Braat, A. Huijser, J. Pasman, G. van Rosmalen, and K. Schouhamer Immink, *Principles of Optical Disc Systems*, Chap. 2, Adam Hilger Ltd, Bristol, 1985.
3. A. Marchant, *Optical Recording-A Technical Overview*, Chap. 5,7, Addison-Wesley, Reading, 1990.
4. M. Mansuripur and C. Pons, "Diffraction Modeling of Optical Path for Magneto-Optical Disk Systems," *Proc. SPIE*, 899, pp. 592-597, 1988.
5. M.V.R.K. Murty, "Lateral Shearing Interferometers," *Optical Shop Testing*, D. Malacara,

Ed., pp. 105-148, John Wiley and Sons, New York, 1978.

6. J.H. McLeod, "The Axicon: A New Type of Optical Element," *JOSA*, **44**, No. 8, pp. 592-597, 1954.

7. J.H. McLeod, "Axicons and Their Uses," *JOSA*, **50**, No. 2, pp. 166-169, 1960.

8. A. Smid, P.F. Ferdinand, and H. 't Lam, "Opto-electronic focussing-error detection system," *European Patent Application*, App. No. 85201588.2, Pub. No. 0 177 108, 1985.

APPENDIX B
